Forest Ecology and Management 541 (2023) 121069

Contents lists available at ScienceDirect

Forest Ecology and Management

journal homepage: www.elsevier.com/locate/foreco

Delineating vulnerability to drought using a process-based growth model in Pyrenean silver fir forests

Cristina Valeriano [a,b,*], Jan Tumajer [c], Antonio Gazol [a], Ester González de Andrés [a], Raúl Sánchez-Salguero [a,d], Michele Colangelo [a,e], Juan C. Linares [d], Teresa Valor [f], Gabriel Sangüesa-Barreda [g], J. Julio Camarero [a]

[a] Instituto Pirenaico de Ecología (CSIC), Avda. Montañana 10005, Zaragoza 50009, Spain
[b] Department of Natural Systems and Resources, Universidad Politécnica de Madrid, Madrid, Spain
[c] Department of Physical Geography and Geoecology, Faculty of Science, Charles University, Albertov 6, 12843 Prague, Czech Republic
[d] Departamento de Sistemas Físicos, Químicos y Naturales, Universidad Pablo de Olavide, Sevilla, Spain
[e] Scuola di Scienze Agrarie, Forestali, Alimentari, e Ambientali, Università della Basilicata, Potenza, Italy
[f] Joint Research Unit CTFC–AGROTECNIO, Solsona, Spain
[g] EiFAB-iuFOR, Universidad de Valladolid, Campus Duques de Soria, 42004 Soria, Spain

ARTICLE INFO

Keywords:
Abies alba
Dendroecology
Drought
Forest dieback
Pyrenees
Vaganov Shashkin

ABSTRACT

Assessing tree growth patterns and deviations from expected climate baselines across wide environmental gradients is fundamental to determine forest vulnerability to drought. This need is particularly compelling for the southernmost limit of the tree species distribution where hot droughts often trigger forest dieback processes. This is the case of some silver fir (*Abies alba*) populations located in southwestern Europe (Spanish Pyrenees) which present ongoing dieback processes since the 1980s. We sampled 21 silver fir stands showing different dieback intensity, assessed using defoliation levels, quantified their growth patterns and characterized their responses to climate. Then, we assessed growth deviations from climatic predictions using the process-based Vaganov-Shashkin (VS) growth model. The forests showing most intense dieback, i.e. highest defoliation levels, were mainly located in low-elevation sites of the western Pyrenees. Trees in these stands displayed the lowest growth rates and the highest year-to-year variability in growth and their growth was limited by late-summer evaporative demand. In eastern and central Pyrenees, we detected a mild growth limitation by low soil moisture during the late growing season and positive growth recovery in recent years with respect to a climate baseline. Decreasing growth trajectories were the most common pattern, while rising trends were common in stands with low dieback in eastern and central Pyrenees. Our results portend systematic spatial variability of growth trends across the Pyrenean silver fir populations forming the south-western distribution limit of the species in Europe. Decoupling of growth between eastern and western populations observed in the recent decades suggests contrasting vulnerability to climate change, and more importantly, the decoupling of growth patterns in western clusters could be used as an early-warning signal of impending dieback. Consequently, we foresee future dieback events to have more detrimental effects in the western compared with the eastern Pyrenees.

1. Introduction

Drought stress has become a crucial constraint of tree growth and vigor worldwide (Williams et al., 2013; Babst et al., 2019). Warmer and drier conditions expose trees to increased evaporative demand (high vapour pressure deficit –VPD) leading to declines in tree radial growth mainly in dry regions but also affecting growth in temperate and mountain forests (Restaino et al., 2016; Sánchez-Salguero et al., 2017a; McDowell et al., 2022). Moreover, increased climate variability can make extreme events such as droughts and heatwaves more frequent and severe (Spinoni et al., 2018).

In Europe, warmer and more variable climate conditions have been

* Corresponding author at: Instituto Pirenaico de Ecología (CSIC)
E-mail addresses: cvaleriano@ipe.csic.es (C. Valeriano), tumajerj@natur.cuni.cz (J. Tumajer), agazolbu@gmail.com (A. Gazol), ester.gonzalez@ipe.csic.es (E. González de Andrés), rsanchez@upo.es (R. Sánchez-Salguero), michelecolangelo3@gmail.com (M. Colangelo), jclincal@upo.es (J.C. Linares), teresa.valor@ctfc.cat (T. Valor), gabriel.sanguesa@uva.es (G. Sangüesa-Barreda), jjcamarero@ipe.csic.es (J. Julio Camarero).

https://doi.org/10.1016/j.foreco.2023.121069
Received 21 February 2023; Received in revised form 28 April 2023; Accepted 30 April 2023
Available online 10 May 2023

linked to increased forest dieback and tree mortality rates (Neumann et al., 2017; Gazol and Camarero 2022, Piedallu et al., 2022). Among European tree species, silver fir (*Abies alba* Mill.) is a key conifer in temperate mountain forests, which has shown different growth patterns and responses to climate across its distribution range (Büntgen et al., 2014; Zang et al., 2014; Gazol et al., 2015; Vitali et al., 2017; Bošela et al., 2018; Vitasse et al., 2019). The distribution of silver fir is expected to shift northwards and upwards according to warmer climate projections, whereas the current range would be substantially reduced in southern Europe in response to warmer-drier conditions (Tinner et al., 2013; Ruosch et al., 2016). Indeed, some populations located in the western Spanish Pyrenees, near the south-western distribution margin of the species in Europe, are showing ongoing dieback processes characterized by growth decline and increasing defoliation and mortality rates (Gazol et al., 2015, 2019; Hernández et al., 2019). This dieback has been related to severe late-summer droughts, warmer temperatures and increased evaporative demand (Camarero et al., 2011; Vicente-Serrano et al., 2015; González de Andrés et al., 2022). Silver fir dieback was also observed in other drought-prone areas, such as south-eastern France (Cailleret et al., 2013; Cailleret and Hendrik, 2011), suggesting widespread decline and mortality under climate warming near the southern distribution limit of the species in Europe. Silver fir is a shade-tolerant species characterized by a high sensitivity to elevated VPD which makes it very vulnerable to warmer climate conditions (Aussenac 2002; Dobrowolska et al., 2017). Therefore, it is unclear to what extent silver fir populations occupying a dry edge of the species range, such as those inhabiting the Spanish Pyrenees, will be able to grow and survive under warmer conditions and increasing evaporative demand (Sánchez-Salguero et al., 2017a; Camarero and Gazol 2022).

Here, we aim to characterize the spatial and temporal variability in the response of silver fir forest to climate. To do so, we used tree-ring data covering a wide longitudinal spatial gradient at the southwestern distribution limit of the species in the Spanish Pyrenees. First, climate and growth patterns were characterized in the study stands. Second, linear climate-growth relationships were calculated to quantify the growth response to climate variables. Third, the Vaganov-Shashkin model (hereafter VS model; Vaganov et al., 2006) was applied to forecast the silver fir growth responses to summer drought stress. We calibrated the VS model using past tree-growth variability. Then, we simulated the expected growth dynamics under current climatic conditions as a baseline. Growth residuals, i.e., differences between observed and VS-simulated growth indices, were used to assess growth tolerance to climatic variability over time. We linked positive residuals to efficient adaptation to drier climatic conditions (e.g., increased water-use efficiency, deeper roots). By contrast, negative residuals were considered as early warning signals of dieback, assuming they reflect a deterioration of drought-avoidance mechanisms (e.g., xylem embolism, carbon starvation). Finally, we compared climate-growth associations among geographical regions that could explain the divergence between observed and predicted growth rates.

The main objectives of the study are: (i) to explore the spatio-temporal patterns of silver fir growth rates, (ii) to assess climate-growth responses using Pearson correlations, and (iii) to obtain VS-model growth residuals. To characterize the common growth patterns among sites and to detect if declining sites were geographically aggregated, cluster analyses were applied. The VS-model residuals are used to foresee the silver fir growth and vigor responses under the forecasted climate warming. In this way, we use the VS-model as an efficient forecasting tool to highlight the variability in vulnerability of temperate mountain forests to drought stress by explicitly considering their spatio-temporal patterns of tree growth and responses to climate.

We hypothesized that declining silver fir sites, i.e., those showing lower growth rates and higher defoliation levels, will be the most sensitive to summer drought and present negative growth residuals, i.e., significant negative deviations of their current growth from the VS-modeled baseline due to pervasive vitality loses. We also expect declining stands will be spatially clustered and located in climatically marginal sites at low elevation, i.e., subjected to warmer and drier conditions in late summer.

2. Materials and methods

2.1. Study area and study species

Silver fir shows a fragmented distribution range across the Spanish Pyrenees (Fig. 1), where the southwestern distribution limit of the species is found (Vitasse et al., 2019). Pyrenean silver fir forests occupy humid and cool sites near valley bottoms or in N to NW-oriented slopes in low-elevation sites of the western Pyrenees, often co-occurring with European beech (*Fagus sylvatica* L.). High-elevation silver fir stands in the central and eastern Pyrenees often coexist with mountain pine (*Pinus uncinata* Ram.). Climate conditions in the Pyrenees change from temperate-oceanic in the west, with cool-wet spring and winter, to Mediterranean in the south and east, with dry summers and moist autumn conditions (Vigo and Ninot 1987).

We studied 21 silver fir stands across the Pyrenees, but mainly located in Spain (Fig. 1). Sites were distributed across a wide altitudinal range (848 to 1800 m a.s.l.) and along a longitudinal gradient (Table 1). The sites were grouped into geographical clusters in the western (11 sites), central (4), and eastern (6) parts of the mountain range according to previous studies (Camarero et al., 2011, 2018, 2018). The temperatures of the coldest months in the year range between −6.4 °C and −0.4 °C, whereas those of the warmest months range between 18.0° and 26.4 °C. The annual precipitation totals vary between 766 and ca. 1800 mm. The geographic, topographic, and climatic characteristics of the stands are presented in Table 1. Several sites recently present symptoms of forest dieback including low growth rates, high mortality and defoliation (Fig. 1). The first dieback symptoms were observed in the 1970 s and mid 1980 s after severe late-summer droughts (Camarero et al., 2000). Some of the populations (e.g., Paco Ezpela, Paco Mayor, Gamueta, Selva de Oza) have been sampled or monitored since 1999–2000 (Camarero et al., 2002, 2003, 2011, 2018; Macias et al., 2006; Peguero-Pina et al., 2007; Linares and Camarero 2012a, 2012b; González de Andrés et al., 2014; Sangüesa-Barreda et al., 2015; Hevia et al., 2019).

2.2. Climate data

Daily mean minimum temperature (Tn), maximum (Tx) temperature and precipitation (Prec) of each site were obtained from the 0.1°-gridded E-OBS v. 24.0e database for the 1970–2020 period (Cornes et al., 2018). Moreover, the annual climate water balance of each site was calculated as the difference between Prec and Potential Evapotranspiration (PET). PET was estimated using the Thornthwaite (1948) equation with the package SPEI (Beguería et al., 2022) in R (R Core Team 2022). We obtained the PET for the hydrological year, from prior October to current September to assess the evaporative demand.

We evaluated the trends of the climatic variables (Tn, Tx, Prec and water balance) for each site using linear regressions. Moreover, we identified trend breakpoints in series of each climatic series and site using the function *TrendAAT* (trend estimation based on annual aggregated time series) from the *greenbrown* R package (Forkel and Wutzler 2015).

2.3. Field sampling

Sampling was performed from 2017 to late 2020 following Camarero et al. (2011). In each site, we selected between 11 and 38 dominant mature trees within a 100-m long and 10-m wide transect randomly located within the stand. We sampled on average 20 trees per stand and 447 in total (Table 2). Tree vigor was assessed using a semi-quantitative scale based on the percentage of crown defoliation and considering five

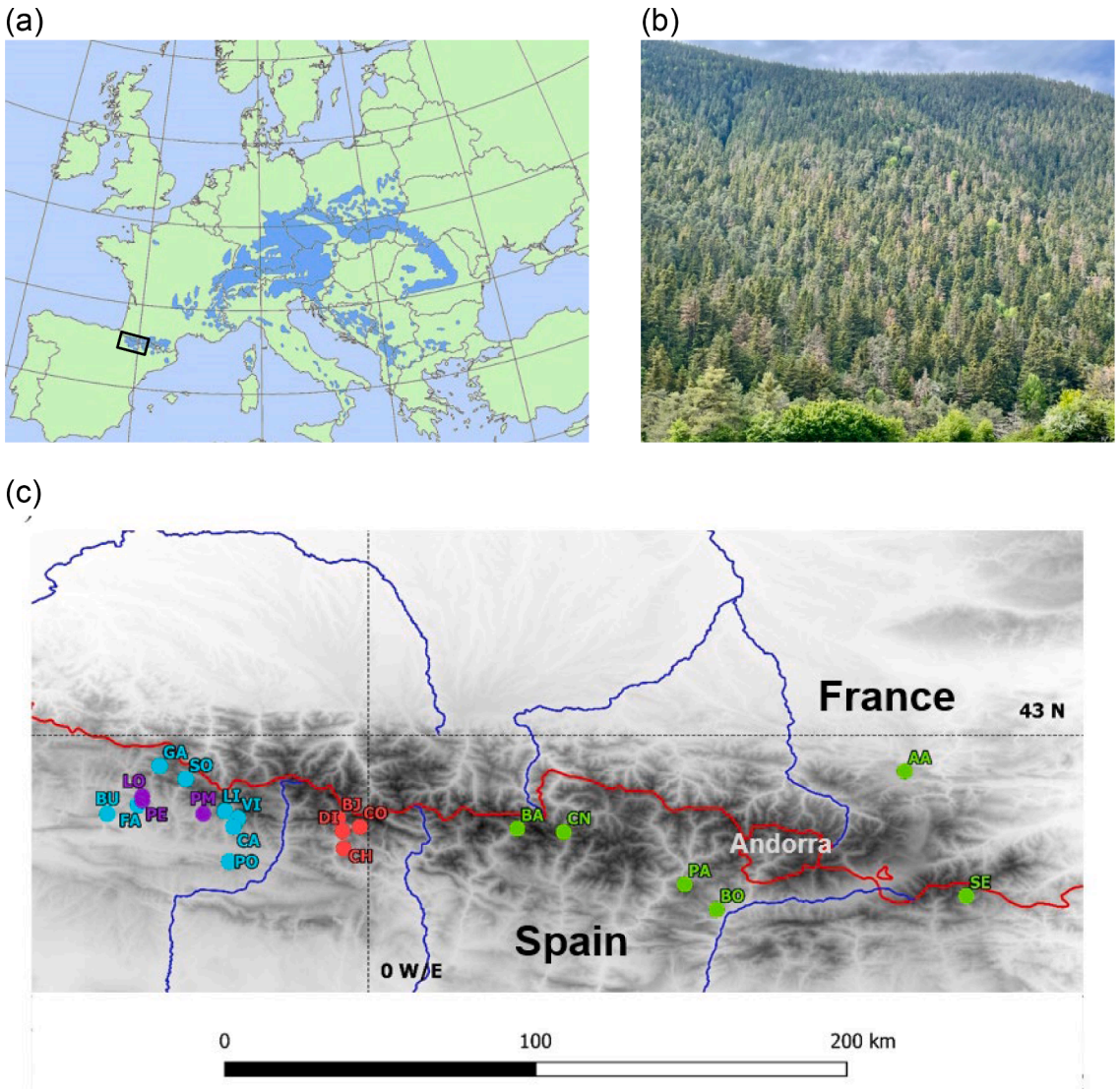

Fig. 1. (a) Distribution range of silver fir (*Abies alba)* in Europe showing the Pyrenees distribution area (rectangle showing the approximate region shown in plot (c)). (b) Picture of the Villanúa (VI site) forest taken in May 2022 showing signs of dieback. (c) Map of the study area in the Pyrenees showing the distribution of the 21 study sites grouped into four different clusters (shown as different colors): West A (blue), West B (purple), Center (red) and East (green) clusters. The background grey scale shows the elevation (from white to black), and the blue lines the major rivers.

classes (Müller and Stierlin, 1990): 0, 0–10% defoliation (healthy tree); 1, 11–25% (slight damage); 2, 26–50% (moderate damage); 3, 51–75% (severe damage); 4, 76–90% (dying tree); and 5, dead trees with > 91% defoliation or only retaining red needles. In each site we used a tree with the maximum amount of foliage for a visual reference. Sites with at least 25% of sampled trees presenting crown defoliation > 50% were considered as declining. Sampling was carried out following standard dendrochronological methods. Specifically, two increment cores per tree were taken at 1.3 m above the stem base and perpendicular to the maximum slope using 5 mm Pressler increment borers (Fritts 1976; Cook and Kairiukstis 1990).

2.4. Tree growth data

Wood samples were air-dried, glued into wooden supports, and polished until the rings could be clearly distinguished. All cores were visually cross-dated, and tree-ring widths (RW) were measured on scanned images (resolution 1200 dpi, EPSON XL 10000) to 0.001 mm precision using the CooRecorder-CDendro software (Larsson and Larsson 2018). The visual cross-dating and measured RW were checked using the software COFECHA (Holmes 1983). Next, RW series from the same tree were averaged together.

We used two approaches to build mean site chronologies based on RW series of individual trees. First, the mean RW series of each tree were transformed into annual basal area increments (BAI) using the following equation and assuming concentric rings:

$$\mathrm{BAI} = \pi(R_t^2 - R_{t-1}^2), \quad (1)$$

where R indicates stem radius and t refers to years. Finally, we averaged BAI from individual series into mean chronologies per each site. In addition, we characterized intra-annual variability in tree growth by means of standardized RW chronologies. To do so, we divided each individual RW series by fitted linear or negative exponential functions to remove long-term trends in growth due to changes in tree size. The first-order autocorrelation of residuals was removed by autoregressive modelling and mean site chronologies of pre-whitened RW indices were obtained using bi-weight robust means. While residual chronologies retained high-frequency variability and removed any longer trends, BAI chronologies reflected both year-to-year and decadal variability. To ensure that growth trends in BAI are not confused with demographic

Table 1
Characteristics of silver fir forests sampled in the Pyrenees. Climate data (mean annual minimum and maximum temperature, sum annual precipitation, and sum annual water balance) correspond to the 1970–2020 period. The column defoliation shows the percentage of trees with crown defoliation higher than 50 %. The last column shows the sites' clusters (W_A, west A; W_B, west B; C, center; E, east) based on their growth series (see Fig. 1).

Site (code)	Latitude N	Longitude –W, +E	Elevation (m)	Min. temp. (°C)	Max. temp. (°C)	Precipitation (mm)	Water balance (mm)	Defoliation (%)	Cluster
Burgui (BU)	42° 42′	−1° 00′	840	−0.9	25.4	884	249	22	W_A
Fago (FA)	42° 44′	−0° 53′	918	−1.7	24.5	819	210	10	W_A
Paco Ezpela (PE)[1]	42° 45′	−0° 52′	1232	−1.7	24.5	865	256	28	W_B
Lopetón (LO)	42° 46′	−0° 52′	1009	−1.7	24.5	894	284	30	W_B
Gamueta (GA)	42° 53′	−0° 48′	1400	−4.4	20.3	1603	699	0	W_A
Selva de Oza (SO)	42° 50′	−0° 42′	1195	−4.7	20.1	1453	680	0	W_A
Paco Mayor (PM)[1]	42° 42′	−0° 38′	1353	−4.3	21.1	924	410	25	W_B
Peña Oroel (PO)	42° 31′	−0° 32′	1587	−1.9	26.4	1191	560	15	W_A
Lierde (LI)	42° 42′	−0° 33′	1222	−4.8	20.5	1194	695	0	W_A
Castiello de Jaca (CA)	42° 39′	−0° 31′	1175	−2.5	24.7	903	305	20	W_A
Paco de Villanúa (VI)	42° 41′	−0° 30′	1234	−4.2	22.2	1194	661	15	W_A
Bujaruelo (BJ)	42° 41′	−0° 07′	1240	−6.4	18.6	1100	577	5	C
Diazas (DI)	42° 38′	−0° 06′	1528	−6.4	18.8	1090	639	0	C
Chate (CH)	42° 34′	−0° 05′	1180	−3.5	23.8	903	332	10	C
Cotatuero (CO)	42° 39′	−0° 03′	1640	−6.4	18.8	1050	599	15	C
Ballibierna (BA)	42° 38′	0° 35′	1600	−6.1	18.0	903	451	0	E
Conangles (CN)	42° 37′	0° 46′	1800	−5.8	18.1	1055	595	0	E
Port Ainé (PA)	42° 25	1° 12′	1740	−4.1	20.1	788	273	0	E
Boumort (BO)	42° 13′	1° 11′	1583	−2.2	23.5	766	155	0	E
Aude (AA)	42° 52′	2° 03′	990	−0.4	23.4	1124	498	15	E
Setcases (SE)	42° 37′	2° 27′	1750	−3.8	19.1	1011	503	0	E

[1] In these two sites, declining (PED, PMD) and non-declining (PEH, PMH) trees were sampled.

Table 2
Descriptive statistics of radial growth series. Sites codes are defined in Table 1. The basal area increment (BAI) trend was calculated since 1970 onwards. Variables' abbreviations: SD, standard deviation; AR1, first-order autocorrelation; MSx, mean sensitivity; EPS, Expressed Population Signal.

Cluster	Site	No. trees	No. radii	Maximum age at 1.3 m (yrs.)	TRW (mm)	SD (mm)	BAI (cm^2)	SD (cm^2)	BAI trend (cm^2 yr^{-1})	AR1	MSx	Period with EPS > 0.85
W_A	BU	11	20	136	3.21	1.48	14.75	1.01	−0.53	0.88	0.17	1968–2017
W_A	FA	25	50	137	2.50	1.01	17.38	0.84	−0.35	0.75	0.21	1888–2019
W_B	PEH	20	37	188	1.45	0.81	9.50	0.74	0.31	0.81	0.26	1920–2019
W_B	PED	19	33	158	1.25	0.68	8.12	0.37	0.05	0.81	0.25	1920–2019
W_B	LO	15	30	133	1.89	0.94	11.43	0.89	0.35	0.83	0.23	1896–2020
W_A	GA	29	59	462	1.52	0.76	21.16	0.65	0.13	0.86	0.20	1810–2019
W_B	SO	20	40	201	2.38	1.10	21.26	0.43	0.04	0.84	0.20	1895–2019
W_B	PMH	19	34	125	1.64	0.98	9.38	0.81	0.36	0.84	0.26	1920–2019
W_B	PMD	19	40	170	1.53	0.93	12.94	0.85	−0.57	0.84	0.25	1920–2019
W_A	PO	12	24	150	1.45	0.58	8.87	0.20	−0.03	0.79	0.20	1870–2019
W_A	LI	34	67	95	3.11	1.36	31.59	0.55	−0.05	0.71	0.20	1868–2017
W_A	CA	17	34	225	1.14	0.68	7.51	0.37	−0.14	0.83	0.23	1893–2017
W_A	VI	33	55	140	1.82	0.85	12.22	0.71	−0.31	0.84	0.25	1892–2017
C	BJ	12	12	99	2.57	1.44	16.35	0.75	−0.31	0.93	0.15	1968–2017
C	DI	16	27	112	2.88	1.22	19.50	0.97	0.33	0.83	0.19	1945–2019
C	CH	11	11	66	2.90	0.88	14.35	0.78	0.32	0.73	0.16	1968–2017
C	CO	15	28	152	1.40	0.60	9.80	0.47	0.14	0.86	0.18	1895–2019
E	BA	32	54	173	2.36	1.05	24.33	0.53	−0.15	0.81	0.18	1894–2018
E	CN	12	12	168	2.76	1.34	28.09	1.31	0.58	0.86	0.20	1868–2017
E	PA	16	31	362	1.60	0.51	12.82	0.30	0.07	0.74	0.17	1895–2019
E	BO	38	66	217	1.93	0.68	14.82	0.64	0.16	0.79	0.21	1871–2020
E	AA	11	13	187	1.90	1.43	24.24	1.58	−0.59	0.87	0.24	1968–2017
E	SE	15	30	79	1.76	1.01	6.83	0.20	−0.07	0.92	0.17	1945–2019

changes in the stand structure, we restricted the use of BAI chronologies to relatively short segments in mature phases of the stand development for calibration of the wood formation model (see chapter 2.7). In total, we built 23 RW chronologies corresponding to 21 sites. In two study sites (PE, PM), we sampled declining and healthy trees and obtained two RW chronologies per site. However, for the individual analyses we selected only the healthy chronology in both sites (Tables 1 and 2). Tree-ring data processing was performed using the dplR package (Bunn 2008, 2010, Bunn et al., 2022).

To characterize and compare chronologies among sites several dendrochronological statistics were calculated, including mean and standard deviation of RW and BAI, first-order autocorrelation (AR1) of RW, which measures year-to-year growth persistence, and mean sensitivity (MSx) of standardized RW indices, which is a relative measure of growth change between consecutive rings (Fritts 1976). The Expressed Population Signal (EPS) was also calculated to assess internal replication and coherence of chronology compared with a theoretical infinitely replicated chronology (Wigley et al., 1984). We considered the threshold of EPS > 0.85 for selecting robust segments of each chronology. Accordingly, all subsequent analyses were restricted to the period 1970–2017/2020 (see Table 2), which is the best-replicated period common to all sites. To evaluate relationships among site mean values (climatic variables, elevation, defoliation, BAI, BAI trend), Pearson (r) or Spearman (r_s) correlations were used for normally and non-normally

distributed variables, respectively.

2.5. Clustering of silver fir chronologies

To characterize the common growth patterns among the 21 study sites, spatially constrained hierarchical cluster analysis and non-hierarchical or partitional clustering were performed. The inputs into both clustering methods included site RW residual chronologies. For the hierarchical clustering, the Ward clustering method was used with the package *Stats* in R (Murtagh and Legendre 2014) in R. The hierarchical clustering was spatially constrained based on the forests' locations. Once each site was assigned to the cluster, we obtained mean annual or daily values of several variables for each cluster (climate variables, BAI, simulated growth indices).

2.6. Climate-growth relationships

To assess climate-growth relationships at the site scale, we calculated the Pearson correlation coefficients between the residual RW chronologies and daily climate data (Tx, Tn and water balance) considering the period 1970–2017/2020. Correlations were calculated for daily climatic data averaged for all possible windows with duration between 30 and 90 days starting from the 1st January of the year before the specific tree-ring formation and ending on the 31st December of tree-ring formation year. The resulting correlations were plotted into a matrix to highlight shifts of climate-growth responses. Correlations were calculated using the *dendrotools* package (Jevšenak & Levanič, 2018) in R. We also assessed how monthly climate variables drove year-to-year growth variability to determine the evolution of the climate response. We calculated for each site Pearson correlation coefficients between the site residual chronologies of RW indices and monthly and seasonal climate data (temperature and precipitation) considering the common period 1970–2020 and two subperiods (1970–2000 and 2001–2020).

2.7. Growth simulations using a process-based model

To produce a baseline of climate-driven growth after 2000 s we simulated the intra-annual growth patterns of each site using the process-based model of wood formation, namely VS model (Vaganov et al., 2006) implemented in the VS-Oscilloscope 1.37 software (Shishov et al., 2016). For each site, we used the daily climate variables (mean temperature, precipitation) and growth data (BAI chronologies). BAI chronologies were preferred for calibration of the VS model of wood formation since they better represent the annual intensity of physiological processes responsible for wood production compared to RW chronologies (Tychkov et al., 2019). We set the cambial parameters of the growth model as constant for all sites, and the rest of the parameters were calibrated for each site (**Table S1**). To do so, we varied all parameters inside their reasonable intervals and selected the combination of parameters that maximized the Pearson correlation coefficient between observed and simulated BAI series and the Gleichläufigkeit statistic, which measures the percentage of common signs in year-to-year growth change (Buras and Wilmking, 2015). The models were calibrated over the period 1970–2000 and, next, run on an independent period since 2001 to validate their temporal stationarity. We assumed that the VS model calibrated during 1970–2000 will produce a baseline of climate-driven growth after 2000 under the assumption that the tree growth responds to climatic variation in an unchanged way. By contrast, systematic deviations of observed BAI series from simulated baselines in verification period should highlight processes driving the decoupling of radial growth from its climatic constraints over time. The VS model assumes non-linear response of radial growth to climate variation and hence it is significantly less sensitive to climate-growth non-stationarity under ongoing climate change compared to traditional linear methods (Tumajer et al. 2023). Therefore, we considered residuals of the model after 2000 as robust signs of health deterioration or adaptation, i.e., processes beyond the mechanisms of regular climate-growth responses. These might include defoliation and dieback (negative residuals) or adaptation through reduced competition or deeper root system (positive residuals). Therefore, we compared mean residuals of the observed BAI chronologies and simulated series after 2000 between sites and clusters.

The VS model simulates daily integral growth rates (Gr) depending on the partial growth rates due to temperature (GrT) or soil moisture (GrM), both reflecting main climatic limiting factors of wood formation. The model focuses on cambial activity and assumes that daily growth rates are non-linearly limited by low temperature (low GrT) or reduced soil moisture (low GrM) depending on specific daily climatic conditions. The limitations due to solar radiation (GrE) depend on site latitude and vary systematically with a day length. We plotted mean intra-annual patterns of limitations for each site due to GrT (high temperature) and GrM (drought). Next, we compared mean pattern of GrM in a known drought year 1985–86 with the years with average climatic conditions preceding and following the event.

3. Results

3.1. Climate trends

Both maximum (r = -0.60, p = 0.004) and minimum (r = -0.57, p = 0.007) temperatures decreased as site elevation increased, but no significant relationship was found between the water balance and site elevation (Table 1). Since the 1970 s, the annual water balance has decreased at a mean rate of -2.11 mm yr^{-1} with a range from -3.40 to -1.60 mm yr^{-1}, while potential evapotranspiration clearly rose after the 1980 s, particularly in the western study area (Fig. 2. **and S1**). Trends in water balance did not differ between geographical clusters. Minimum and maximum temperatures increased in all sites at mean rates of + 0.08 °C yr^{-1} and + 0.01 °C yr^{-1}, respectively (**Fig. S1**). The rates of minimum temperature increase were positively related to site longitude (r = 0.61, p = 0.003), whereas the rates of maximum temperature increase were negatively related to site latitude ($r = -0.44$, $p = 0.047$). We found trend breakpoints of minimum temperatures in 1986 and 1998 for all silver-fir clusters excepting the east cluster, which only showed a significant trend change in 1998 (**Fig. S2**). Water balance trends showed significant relationship with site latitude ($r = 0.88$, $p < 0.001$), longitude ($r = -0.47$, $p < 0.05$) and elevation ($r = -0.63$, $p < 0.01$) (**Fig. S3**).

3.2. Growth patterns of Pyrenean silver fir forests

The mean age at 1.3 m of sampled trees was 172 years with a range from 66 (Chate) to 462 years (Gamueta). The mean (±SD) BAI was 16.11 (±4.73) cm^2. The mean AR1 and MSx were 0.82 ± 0.06 and 0.20 ± 0.03, respectively. The mean BAI value of each site was positively correlated with the site water balance (r = 0.43, p = 0.05), but negatively related to the site defoliation (r_s = -0.58, p = 0.006). Site defoliation increased as site mean maximum temperature did (r_s = 0.66, p = 0.001; Table 1). Furthermore, the site MSx and defoliation were positively associated (r_s = 0.48, p = 0.03), i.e., declining sites with more defoliated trees showed a higher year-to-year variability in growth (Table 2**, Fig. S4**).

The clustering analyses confirmed systematic differences between residual chronologies between western, central, and eastern cluster (**Fig. S5**). Moreover, it also highlighted significant heterogeneity inside the western cluster. The clustering analysis clearly differentiated between the eight sites with moderate growth decline (west A cluster) and the three sites with the highest defoliation levels across entire Pyrenees with steep growth increase in 2000s followed by a steady decline (west B cluster; Paco Ezpela, Lopetón and Paco Mayor; Table 1).

3.3. Climate-growth relationships

The daily climate-growth correlations revealed differences between

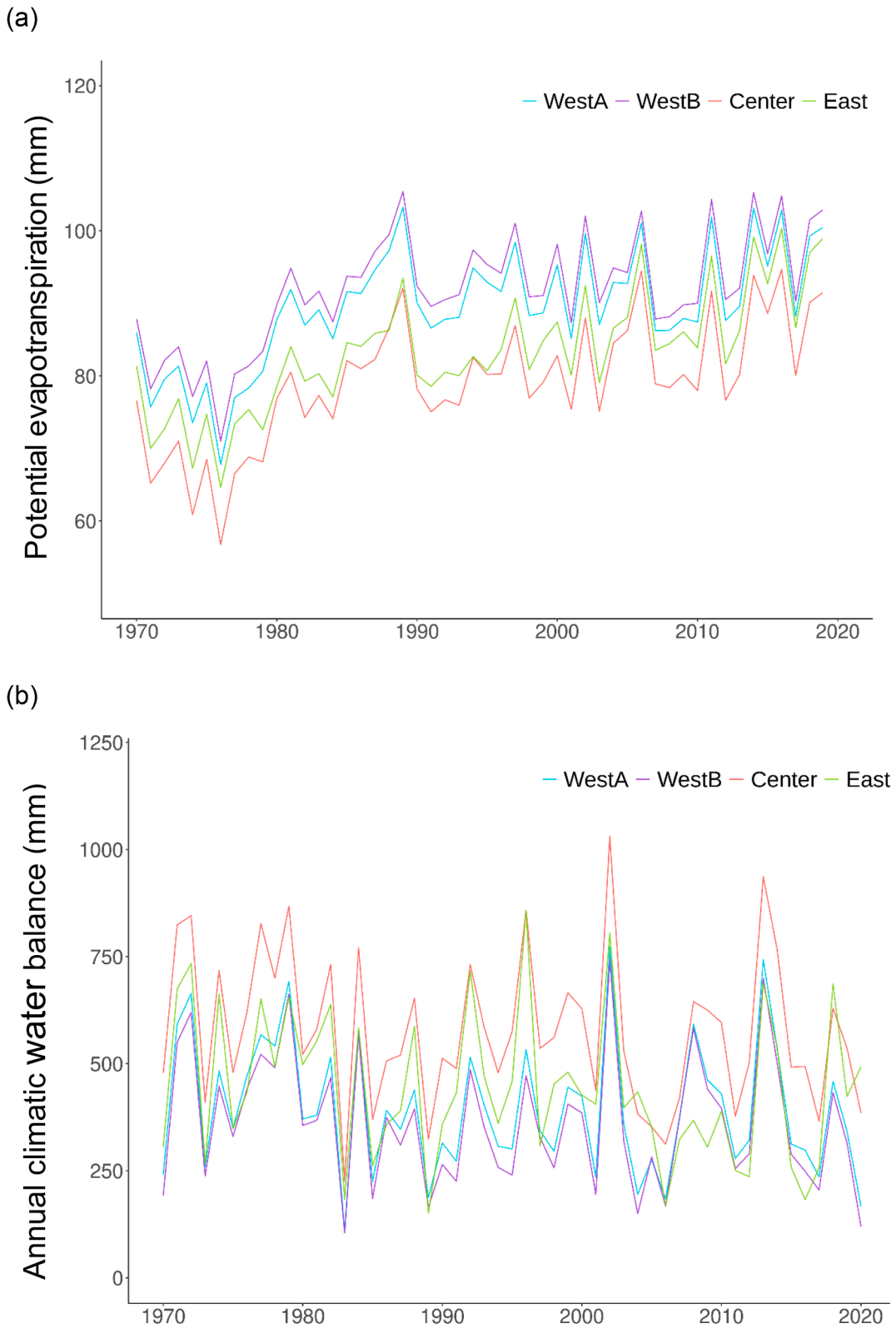

Fig. 2. Potential evapotranspiration of the hydrological year (a) and annual climatic water balance (b) for the four silver-fir clusters from 1970 to 2020.

geographical clusters (Fig. 3). Western sites showed stronger climate-growth correlations compared with central and eastern sites. In the west B cluster, where dieback is intense, the positive responses to prior-summer and current June climate water balance were more marked than in any other cluster. Several sites from the western clusters were characterized by negative responses to high maximum temperatures in the prior late summer and current early summer. Only few sites with low defoliation levels in the eastern cluster showed climate-growth responses to maximum temperatures and water balance comparable to the western clusters (e.g., Ballibierna, Conangles). Several sites from the west (Burgui, Castiello de Jaca, Villanúa) and center (Cotatuero) clusters showed negative responses to minimum temperatures. The monthly

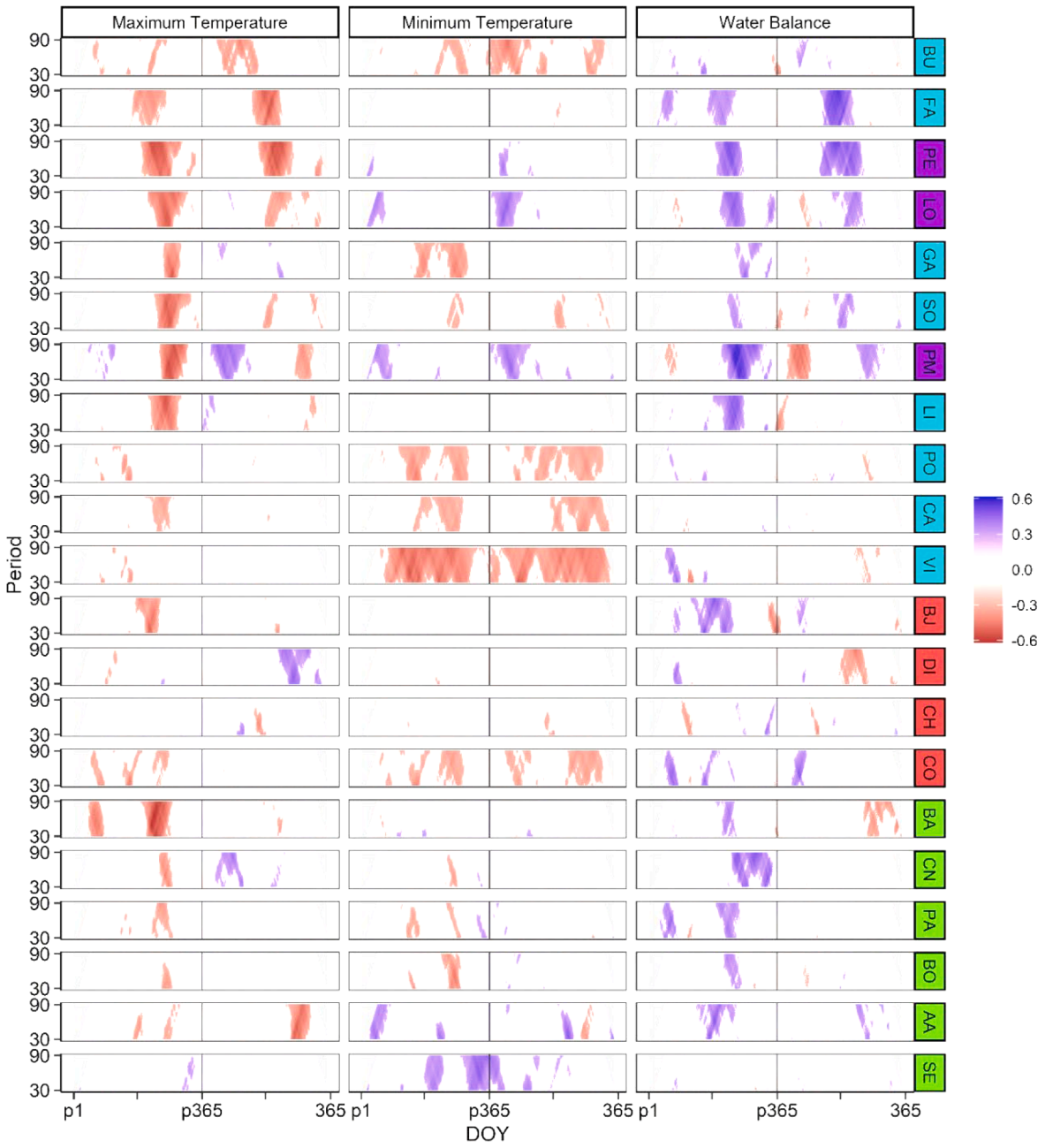

Fig. 3. Climate-growth correlations between mean ring-width chronologies and daily minimum air temperature, maximum air temperature, and water balance in 21 silver-fir sites (period 1970–2020). Climate data were aggregated for windows with duration between 30 and 90 days. The y axes indicate the duration of the aggregation period in days, whereas the × axes indicate the center of the aggregation window. The 'p' letter indicates aggregation windows whose center corresponds to days of the year preceding to the year of the tree-ring formation. Sites are ordered according to their longitude from West to East and are colored as the four clusters shown in Fig. 1c.

growth-climate relationships showed a loss of sensitivity in 2001–2020 as compared with 1970–2000 (**Fig. S6**).

3.4. Simulated intra-annual growth patterns and inferred climate constraints

In the calibration period (1970–2000), significant correlations were obtained between observed and simulated BAI series for all sites (**Table S2**, Fig. 4). However, in the verification period (2001–2017/2020) some sites presented non-significant (e.g., Cotatuero, Boumort, Setcases) or even negative correlations (Ballibierna, Conangles, Port Ainé) (**Table S2**). The correlations during the verification period were high for sites from the western clusters but they dropped towards the eastern parts of Pyrenees.

Mean simulated intra-annual growth rates indicated that low soil moisture constrained silver fir growth mainly in the west A and B clusters. In all clusters, growth was limited by both low winter temperatures and summer/autumn drought stress according to VS-model simulations (Fig. 5 **and S7**). The growth limitation by water shortage was confirmed when considering the severe 1985–1986 drought, when soil moisture clearly constrained silver fir growth in the west A and B clusters (**Fig. S8**).

3.5. Recent divergence between observed and simulated growth

Residuals between observed BAI chronologies and simulations

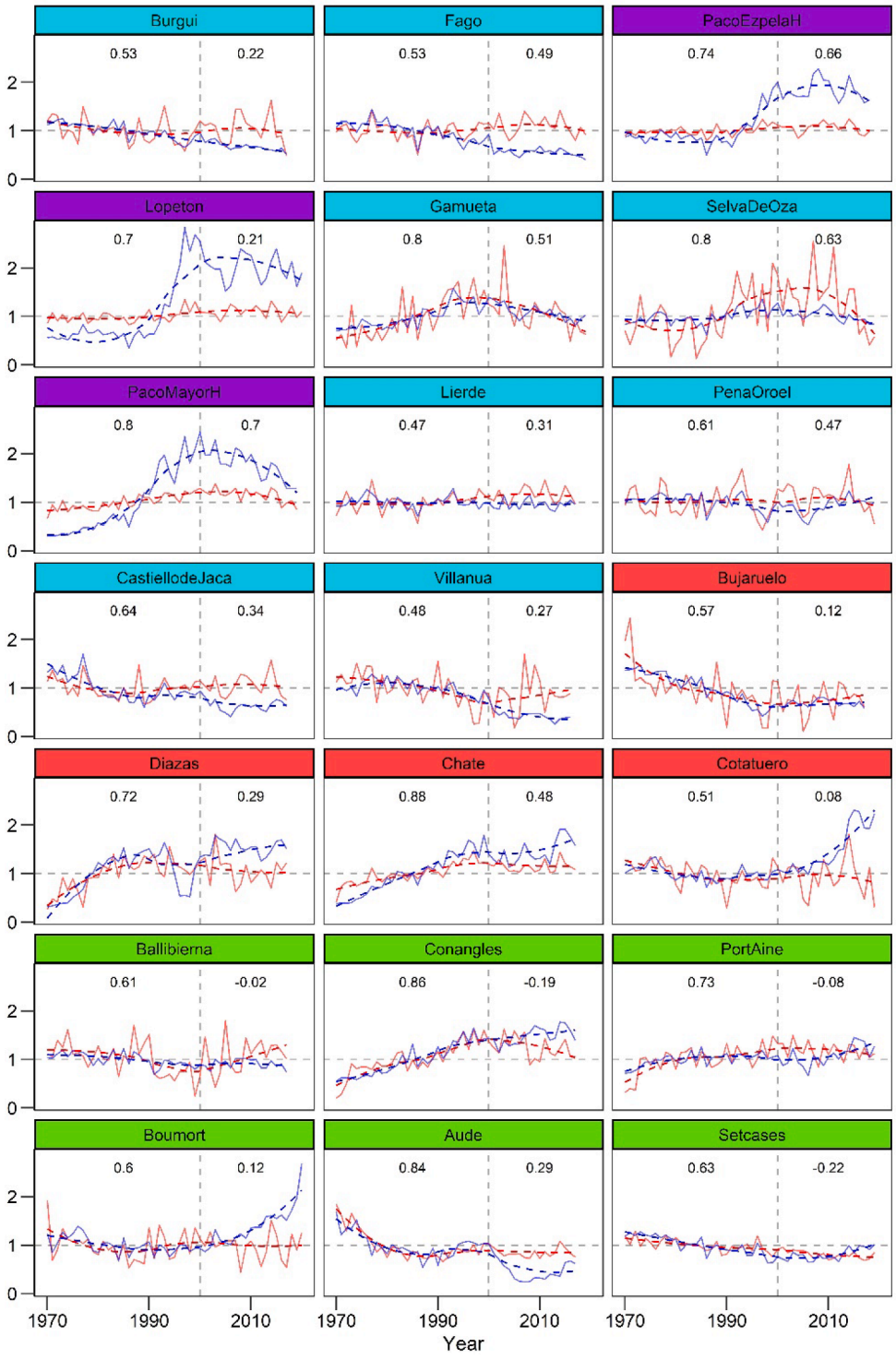

Fig. 4. Simulated (red lines) and observed (blue lines) basal area increment (BAI) series for each site. The VS model was fitted considering the period 1970–2000 and then used to simulate growth after 2001 (dashed vertical lines separate both periods). Continuous blue and red lines show observed and simulated BAI series, respectively, and dashed lines their smoothed values. Values on top of the charts indicate Pearson correlations between simulated chronologies for calibration (1970–2000) and verification periods (since 2001). Observed and simulated BAI series were standardized (values in y axes).

showed slightly declining trends in the west A cluster since 2000s. By contrast, a sharp increase in residuals was observed in the west B cluster around 2000s followed by a steady decline afterwards. In the center and east clusters, the increase of BAI residuals after 2000s was moderate. Chronologies based on declining trees showed more negative residuals compared to their clusters' means both in the west A and east clusters (Fig. 6).

4. Discussion

Forest dieback in silver fir western Pyrenean stands is ongoing as climate conditions become warmer and drier, mainly affecting low-elevation sites (Camarero et al 2011; Gazol et al. 2023). We found the highest defoliation levels in sites from the west B cluster, where linear climate-growth correlations showed a tight coupling of radial growth with climate variability. By contrast, the drought limitation was weaker in the eastern part of the Pyrenees, where climate constrains to a lesser extent tree growth. In agreement with observed defoliation levels, some

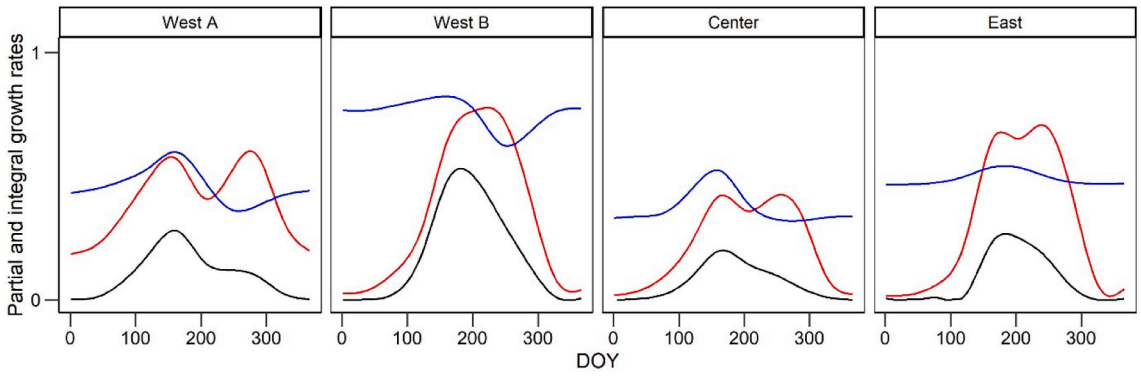

Fig. 5. Simulated partial and integral (black lines) growth rates obtained from the VS model averaged in the four silver-fir clusters (West A, West B, Center and East) for the period 1970–2000. The partial growth rates correspond to growth limitations due to temperature (red lines) or soil moisture availability (blue lines). The higher the value of partial growth rate, the less limiting effect of given climatic variable on radial wood formation. Integral growth rate is the simulated rate of radial growth with higher values of integral growth rate indicating faster radial growth. DOY is the day of the year.

sites in the western A cluster (e.g., BU, CA and VI) showed recent negative BAI deviations from the simulated baseline. This deviation and the increasing defoliation and mortality rates suggest forest dieback would aggravate in these stands. By contrast, the growth trends observed within central and eastern sites exceeded baseline simulation, suggesting improved responses to changing environment or less stressful conditions during a warming hiatus (Ballantyne et al., 2017). We consider that the residuals between modeled and observed BAI reflect processes that might potentially lead to future forest dieback events as illustrated in the western cluster by observed high levels of defoliation in agreement with negative residuals.

The geographical pattern of strong silver fir dieback in the western Pyrenees and relatively healthy and vigorous stands in eastern Pyrenees could be explained by at least two factors. First, the seasonal distribution of precipitation is different across the range with higher winter-spring precipitation in the west unlike the higher summer-fall precipitation in the east which could alleviate summer drought stress (Camarero et al., 2011). Moreover, maximum temperatures grew more rapidly in western sites since 1970s, whereas minimum temperatures increased more in eastern than in western Pyrenean sites. Accordingly, climate water balance has decreased more in low-elevation western sites subjected to increasingly warmer conditions. In a recent study, Zweifel et al. (2021) found that silver fir had greater intra-annual growth rates than other species because its capacity to initiate growth early at night Higher temperatures and VPD, and less humidity, in sun exposed western silver fir forests such as Paco Ezpela or Paco Mayor can substantially reduce water availability, impairing growing hours during nighttime, thus resulting in low growth rates. Second, western silver fir populations are genetically less adapted to tolerate summer drought than eastern populations due to the westward post-glacial migration of the species (Matías et al., 2016). The importance of different post-glacial histories for the growth sensitivity of silver fir populations to summer drought has already been revealed in studies across several European regions (Bošela et al., 2016; Vitali et al., 2017). Future research should verify contribution of genetic predispositions and indirect effects of management legacies to tolerance of summer atmospheric drought in western and eastern Pyrenean silver fir lineages.

Our results depict important implication regarding the observed differences between eastern and western populations for the future responses of silver fir to ongoing climate change. The post-2000 BAI residuals were mainly negative in the western part, but steady or positive in eastern and central parts of mountain range. This regional pattern suggests contrasting vulnerability of silver fir to cope with climate change. Current growth in the western region lacks behind the climatic baseline suggesting possible physiological weakening following long-term climate dryness (Gazol et al., 2015). Despite the VS model did not account for indirect effects of warmer conditions, as regards increased evaporative demand (rising VPD), it was able to pinpoint sites most vulnerable to water shortage, which show dieback and lowest vigor levels. Other frameworks considering eco-hydrological models could be combined with the VS model to identify VPD thresholds leading to growth decline and dieback in silver fir (Vicente-Serrano et al., 2015).

Sites showing dieback (high defoliation levels, low BAI values) in the western part of Pyrenees seem to be particularly sensitive to water deficit in the previous late summer and the current growing season, according to data of wood density, tree ring nutrients and intrinsic water-use efficiency (Camarero and Gutiérrez 2007; Linares and Camarero 2012b; Hevia et al., 2019; González de Andrés et al., 2022). Further, we observed significantly stronger climate-growth correlations for western sites, where tree growth is probably close to its physiological limits due to harsh drought stress. By opposite, the eastern Pyrenees provides mild climatic conditions, where the effect of ongoing climate change may be buffered (Sánchez-Salguero et al., 2017b). Sites with highest defoliation levels and low growth rates (BAI) from the west B cluster also showed a higher year-to-year variability in growth. However, the interpretation of the rise in non-climatic growth residuals in that region with the highest dieback incidence is not straightforward. Growth releases might be interpreted as a recovery signal induced by stand thinning following mortality events and may be related to the loss of growth responsiveness to climate since the 2000 s (Gazol et al., 2023). Overall, previous studies have demonstrated that growth variability provides an early-warning signal of dieback and impeding mortality in those remaining trees (Camarero et al., 2011, 2015; Sangüesa-Barreda et al., 2015).

This research illustrates the spatial variability of silver fir growth trends in the Pyrenees. Our results highlight a decoupling of growth between eastern and western populations in the recent decades, supporting contrasting climate sensitivity an enhanced vulnerability to climate change towards the west of the mountain range. It should be noted, however, that warming trends has been less intense during the last decades (Ballantyne et al., 2017). This can explain divergent patterns because in those sites where climate has surpassed fir's tolerance limits (i.e. western sites) the amelioration of warming has no beneficial impacts (Sánchez-Salguero et al., 2017b). Conversely, in central sites the less intense warming may have favored growth recovery and stimulate it by extension of growing season and faster cambial kinetics in spring. We foresee that future events such as recurring droughts will have more detrimental effects in the western compared to the eastern silver-fir stands of the Spanish Pyrenees.

5. Conclusions

The clustering of tree-ring width chronologies helped to disentangle the spatial patterns of silver fir dieback, which was characterized by

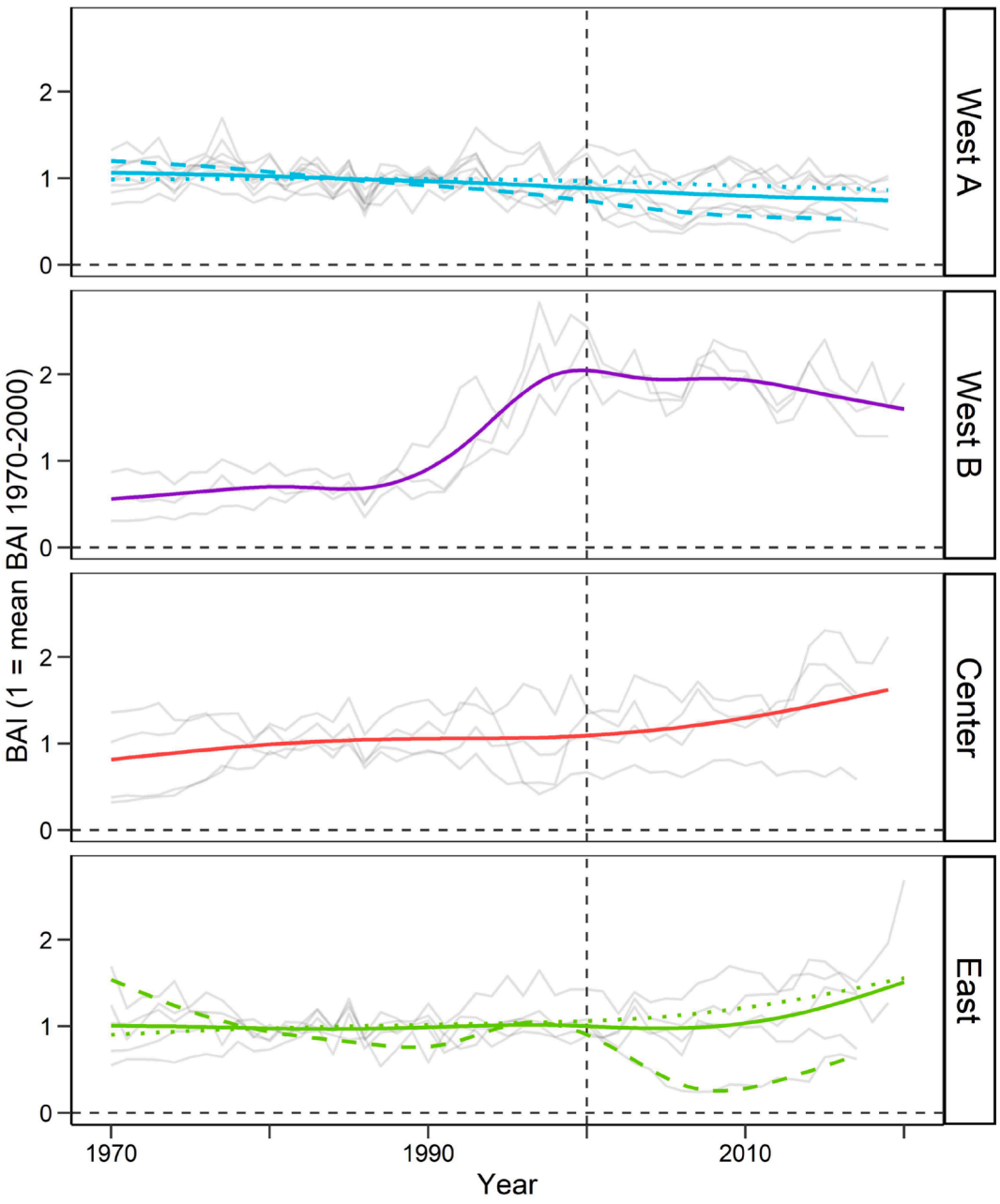

Fig. 6. Residuals of basal area increment (BAI) (differences between observed BAI series and simulated BAI series produced by the VS model) calculated in the four silver-fir clusters. Grey lines show residuals for individual sites, and color lines are smoothed values for mean of cluster. In the west A and east clusters, dotted lines are non-declining sites and dashed lines are declining sites. The dashed vertical line indicates the 2000 year when minimum temperatures started to sharply increase. We also used 2000 as the end of the VS model calibration period.

high defoliation levels, low growth rates and growth below the simulated baseline since 2000s in low-elevation sites from the western Pyrenees subjected to increasingly warmer conditions. Climate-growth correlations confirmed that silver fir dieback was triggered by a negative water balance during the previous late summer and by low soil moisture levels during the current late growing season. Sites showing dieback are probably vulnerable to both sources of climate stress. The presented framework using the VS model of wood formation allowed linking current dieback extent with the decoupling of observed and simulated tree-ring width indices. The use of the VS model to calculate growth deviations with respect to a climate baseline could be further explored to: (i) evaluate post-dieback growth recovery, and (ii) detect emerging dieback hotspots.

CRediT authorship contribution statement

Cristina Valeriano: Conceptualization, Methodology, Data curation, Formal analysis, Writing – original draft, Writing – review & editing. **Jan Tumajer:** Methodology, Data curation, Validation, Formal analysis, Writing – original draft, Writing – review & editing. **Antonio Gazol:** Conceptualization, Data curation, Writing – review & editing. **Ester González de Andrés:** Methodology, Writing – review & editing. **Raúl Sánchez-Salguero:** Conceptualization, Data curation, Writing – review & editing. **Michele Colangelo:** Methodology, Writing – review & editing. **Juan C. Linares:** Conceptualization, Writing – review & editing. **Teresa Valor:** Writing – review & editing. **Gabriel Sangüesa-Barreda:** Conceptualization, Writing – review & editing. **J. Julio Camarero:** Conceptualization, Data curation, Funding acquisition, Writing – review

& editing.

Declaration of Competing Interest

The authors declare that they have no known competing financial interests or personal relationships that could have appeared to influence the work reported in this paper.

Data availability

Data will be made available on request.

Acknowledgments

We thank the Aragón Government for its continuous support on this research. We thank Pere Casals and Lena Vila for their help during the field work. We also thank the following projects funded by the Spanish Ministry of Economy (CGL2015-69186-C2-1-R) and the Spanish Ministry of Science, Innovation and Universities (RTI2018-096884-B-C31). C. Valeriano acknowledges funding by a FPI grant (PRE2019-089800) associated to project RTI2018-096884-B-C31. J. Tumajer was supported by Charles University (UNCE HUM/018). A. Gazol is supported by the Ramón y Cajal Program of the Spanish MICINN under Grant RyC2020-030647-I, and by CSIC and Science and Innovation Ministry under grants PIE-20223AT003 and PID2021-123675OB-C43, respectively, also by TED2021-129770B-C21. G. Sangüesa-Barreda was supported by a Postdoctoral grant (IJC2019-040571-I) funded by MCIN/AEI /10.13039/501100011033. R. Sánchez-Salguero and JC. Linares were supported by VULBOS (UPO-1263216) and VURECLIM (P20_00813) projects, both by FEDER Funds, Andalusia Regional Government, Consejería de Economía, Conocimiento, Empresas y Universidad 2014-2020; and supported by EQC2018-004821-P and IE19_074 UPO projects cofounded by Spanish "Plan Estatal de Investigación Científica y Técnica y de Innovación 2017-2020" and Plan Andaluz de Invetigación, Desarrollo e Innovación (PAIDI 2020). We thank two anonymous reviewers for their stimulating comments about the earlier version of the manuscript.

Appendix A. Supplementary material

Supplementary data to this article can be found online at https://doi.org/10.1016/j.foreco.2023.121069.

References

Aussenac, G., 2002. Ecology and ecophysiology of circum-Mediterranean firs in the context of climate change. Ann. For. Sci. 59, 823–832. https://doi.org/10.1051/forest:2002080.

Babst, F., Bouriaud, O., Poulter, B., Trouet, V., Girardin, M.P., Frank, D.C., 2019. Twentieth century redistribution in climatic drivers of global tree growth. ScienceAdvances 5, eaat4313. https://doi.org/10.1126/sciadv.aat4313.

Ballantyne, A., Smith, W., Anderegg, W., Ballantyne, A., Smith, W., Anderegg, W., Kauppi, P., Sarmiento, J., Tans, P., Running, S., 2017. Accelerating net terrestrial carbon uptake during the warming hiatus due to reduced respiration. Nature Clim Change 7, 148–152. https://doi.org/10.1038/nclimate3204.

Beguería, S., Vicente Serrano, S.M., Reig-Gracia, F., Latorre Garcés, B. 2022. SPEIbase v.2.7 ; DIGITAL.CSIC; Version 2.7, doi: 10.20350/digitalCSIC/14612.

Bošela, M., Popa, I., Gömöry, D., Longauer, R., Tobin, B., et al., 2016. Effects of post-glacial phylogeny and genetic diversity on the growth variability and climate sensitivity of European silver fir. Glob. Ch. Biol. 104, 716–724. https://doi.org/10.1111/1365-2745.12561.

Bošela, M., Lukac, M., Castagneri, D., Sedmák, R., Biber, P., Carrer, M., Konôpka, B., Nola, P., Nagel, A.T., Popa, I., et al., 2018. Contrasting effects of environmental change on the radial growth of co-occurring beech and fir trees across Europe. Sci. Tot. Env. 615, 1460–1469. https://doi.org/10.1016/j.scitotenv.2017.09.092.

Bunn, A.G., 2008. A dendrochronology program library in R (dplR). Dendrochronologia 26, 115–124.

Bunn, A.G., 2010. Statistical and visual crossdating in R using the dplR library. Dendrochronologia 28, 251–258.

Bunn A, Korpela M, Biondi F, Campelo F, Mérian P, Qeadan F, Zang C. 2022. dplR: Dendrochronology Program Library in R. R package version 1.7.4, https://CRAN.R-project.org/package=dplR.

Büntgen, U., Tegel, W., Kaplan, J.O., Schaub, M., Hagedorn, F., et al., 2014. Placing unprecedented recent fir growth in a European-wide and Holocene-long context. Front. Ecol. Env. 12, 100–106. https://doi.org/10.1890/130089.

Buras, A., Wilmking, M., 2015. Correcting the calculation of Gleichläufigkeit. Dendrochronologia 34, 29–30. https://doi.org/10.1016/j.dendro.2015.03.003.

Cailleret, M., Hendrik, D., 2011. Effects of climate on diameter growth of co-occurring *Fagus sylvatica* and *Abies alba* along an altitudinal gradient. Trees-Struct. Funct. 25, 265–276. https://doi.org/10.1007/s00468-010-0503-0.

Cailleret, M., Nourtier, M., Amm, A., Durand-Gillmann, M., Davi, H., 2013. Drought-induced decline and mortality of silver fir differ among three sites in Southern France. Ann. For. Sci. 71, 643–657. https://doi.org/10.1007/s13595-013-0265-0.

Camarero, J.J., Martín, E., Gil-Pelegrín, E., 2003. The impact of a needle miner (*Epinotia subsequana*) outbreak on radial growth of silver fir (*Abies alba*) in the Aragón Pyrenees: a dendrochronological assessment. Dendrochronologia 21, 3–12.

Camarero, J.J., Bigler, C., Linares, J.C., Gil-Pelegrín, E., 2011. Synergistic effects of past historical logging and drought on the decline of Pyrenean silver fir forests. For. Ecol. Manage. 262, 759–769. https://doi.org/10.1016/j.foreco.2011.05.009.

Camarero, J.J., Gutiérrez, E., Fortin, M. J., 2000. Spatial pattern of subalpine forest-alpine grassland ecotones in the Spanish Central Pyrenees. Forest Ecology and Management, *134*(1-3), 1-16. https://doi.org/10.1016/S0378-1127(99)00241-8.

Camarero, J.J., Gutiérrez, E., 2007. Response of Pinus uncinata recruitment to climate warming and changes in grazing pressure in an isolated population of the Iberian System (NE Spain). Arctic, Antarctic and Alpine Research 39, 210–217.

Camarero, J.J., Gazol, A., Sangüesa-Barreda, G., Oliva, J., Vicente-Serrano, S.M., 2015. To die or not to die: early warnings of tree dieback in response to a severe drought. J. Ecol. 103, 44–57. https://doi.org/10.1111/1365-2745.12295.

Camarero, J.J., Gazol, A., Sangüesa-Barreda, G., Cantero, A., Sánchez-Salguero, R., Sánchez-Miranda, A., Granda, E., Serra-Maluquer, X., Ibáñez, R., 2018. Forest growth responses to drought at short- and long-term scales in Spain: squeezing the stress memory from tree rings. Front. Ecol. Evol. 6, 9. https://doi.org/10.3389/fevo.2018.00009.

Camarero, J.J., Gazol, A., 2022. Will silver fir be under higher risk due to drought? A comment on Walder et al., (2021). For. Ecol. Manage. 503, 119826 https://doi.org/10.1016/j.foreco.2021.119826.

Camarero, J.J., Padró, A., Martín-Bernal, E., Gil-Pelegrín, E., 2002. Aproximación dendroecológica al decaimiento del abeto (*Abies alba* Mill.) en el Pirineo aragonés. Montes 70, 26–33.

Cook, E.R., Kairiukstis, L.A., 1990. Methods of dendrochronology: application in the environmental sciences. Kluwer, Dordrecht.

Cornes, R.C., van der Schrier, G., van den Besselaar, E.J., Jones, P.D., 2018. An ensemble version of the E-OBS temperature and precipitation data sets. Journal of Geophysical Research: Atmospheres 123 (17), 9391–9409.

Dobrowolska, D., Bončina, A., Klumpp, R., 2017. Ecology and silviculture of silver fir (*Abies alba* Mill.): A review. J. For. Res. 22, 326–335. https://doi.org/10.1080/13416979.2017.1386021.

Forkel M, Wutzler T. 2015. Greenbrown –land surface phenology and trend analysis. A package for the R software. Version 2.2, 2015-04-15, http://greenbrown.r-forge.r-project.org/.

Fritts, H.C., 1976. Tree rings and climate. Academic Press, London, UK.

Gazol, A., Camarero, J.J., Gutiérrez, E., Popa, I., Andreu-Hayles, L., et al., 2015. Distinct effects of climate warming on populations of silver fir (*Abies alba*) across Europe. J. Biogeogr. 42, 1150–1162. https://doi.org/10.1111/jbi.12512.

Gazol, A., Camarero, J.J., Colangelo, M., de Luis, M., Martínez del Castillo, E., Serra-Maluquer, X., 2019. Summer drought and spring frost, but not their interaction, constrain European beech and Silver fir growth in their southern distribution limits. Agric. For. Meteorol. 278, 107695 https://doi.org/10.1016/j.agrformet.2019.107695.

Gazol, A., Camarero, J.J., 2022. Compound climate events increase tree drought mortality across European forests. Sci. Tot. Env. 816, 151604 https://doi.org/10.1016/j.scitotenv.2021.151604.

Gazol, A., González de Andrés, E., Colangelo, M., Valeriano, C., Camarero, J.J., 2023. Pyrenean silver fir forests retain legacies of past disturbances and climate change in their growth, structure and composition. Forests 14, 713.

González de Andrés, E., Camarero, J.J., Martínez, I., Coll, L.l., 2014. Uncoupled spatiotemporal patterns of seed dispersal and regeneration in Pyrenean silver fir populations. For. Ecol. Manage. 319, 18–28. https://doi.org/10.1016/j.foreco.2014.01.050.

González de Andrés, E., Gazol, A., Querejeta, J.I., Igual, J.M., Colangelo, M., et al., 2022. The role of nutritional impairment in carbon-water balance of silver fir drought-induced dieback. Glob. Ch. Biol. 28, 4439–4458. https://doi.org/10.1111/gcb.16170.

Hernández, L., Camarero, J.J., Gil-Peregrín, E., Saz Sánchez, M.Á., Cañellas, I., Montes, F., 2019. Biotic factors and increasing aridity shape the altitudinal shifts of marginal Pyrenean silver fir populations in Europe. For. Ecol. Manage. 432, 558–567. https://doi.org/10.1016/j.foreco.2018.09.037.

Hevia, A., Sánchez-Salguero, R., Camarero, J.J., Querejeta, J.I., Sangüesa-Barreda, G., Gazol, A., 2019. Long-term nutrient imbalances linked to drought-triggered forest dieback. Sci. Tot. Env. 690, 1254–1267. https://doi.org/10.1016/j.scitotenv.2019.06.515.

Holmes, R., 1983. Computer-assisted quality control in tree-ring dating and measurement. Tree Ring Bull. 43, 69–78.

Jevšenak, J., Levanič, T., 2018. dendroTools: R package for studying linear and nonlinear responses between tree-rings and daily environmental data. Dendrochronologia 48, 32–39. https://doi.org/10.1016/j.dendro.2018.01.005.

Larsson L., Larsson P. 2018 CooRecorder / CDendro package version 9.3.1. Cybis, Saltsjöbaden, Sweden.

Linares, J.C., Camarero, J.J., 2012a. Growth patterns and sensitivity to climate predict silver fir decline in the Spanish Pyrenees. Eur. J. For. Res. 131, 1001–1012. https://doi.org/10.1007/s10342-011-0572-7.

Linares, J.C., Camarero, J.J., 2012b. From pattern to process: linking intrinsic water-use efficiency to drought-induced forest decline. Glob. Ch. Biol. 18, 1000–1015. https://doi.org/10.1111/j.1365-2486.2011.02566.x.

Macias, M., Andreu, L., Bosch, O., Camarero, J.J., Gutiérrez, E., 2006. Increasing aridity is enhancing silver fir (*Abies alba* Mill.) water stress in its south-western distribution limit. Clim. Ch. 79, 289–313. https://doi.org/10.1007/s10584-006-9071-0.

Matías, L., González-Díaz, P., Quero, J.L., Camarero, J.J., Lloret, F., Jump, A.S., 2016. Role of geographical provenance in the response of silver fir seedlings to experimental warming and drought. Tree Physiol. 36, 1236–1246. https://doi.org/10.1093/treephys/tpw049.

McDowell, N.G., Sapes, G., Pivovaroff, A., Adams, H.D., Allen, C.D., Anderegg, W.R.L., Arend, M., Breshears, D.D., Brodribb, T., Choat, B., Cochard, H., De Cáceres, M., De Kauwe, M.G., Grossiord, C., Hammond, W.M., Hartmann, H., Hoch, G., Kahmen, A., Klein, T., Xu, C., 2022. Mechanisms of woody-plant mortality under rising drought, CO2 and vapour pressure deficit. Nat. Rev. Earth Environ. 3, 294–308. https://doi.org/10.1038/s43017-022-00272-1.

Müller, E.H.R., Stierlin, H.R., 1990. Sanasilva tree crown photos with percentages of foliage loss. WSL, Birmensdorf, Switzerland.

Murtagh, F., Legendre, P., 2014. Ward's hierarchical agglomerative clustering method: which algorithms implement Ward's criterion? J. Classif. 31, 274–295. https://doi.org/10.1007/s00357-014-9161-z.

Neumann, M., Mues, V., Moreno, A., Hasenauer, H., Seidl, R., 2017. Climate variability drives recent tree mortality in Europe. Glob. Ch. Biol. 23, 4788–4797. https://doi.org/10.1111/gcb.13724.

Peguero-Pina, J.J., Camarero, J.J., Abadía, A., Martín, E., González-Cascón, R., et al., 2007. Physiological performance of silver-fir (*Abies alba* Mill.) populations under contrasting climates near the south-western distribution limit of the species. Flora 202, 226–236. https://doi.org/10.1016/j.flora.2006.06.004.

Piedallu, C., Dallery, D., Bresson, C., Legay, M., Gégout, J.C., Pierrat, R., 2022. Spatial vulnerability assessment of silver fir and Norway spruce dieback driven by climate warming. Landsc. Ecol. https://doi.org/10.1007/s10980-022-01570-1.

R Development Core Team. 2022. R: A Language and Environment for Statistical Computing.

Restaino, C.M., Peterson, D.L., Littell, J., 2016. Increased water deficit decreases Douglas fir growth throughout western US forests. Proc. Natl. Acad. Sci. USA 113, 9557–9562. https://doi.org/10.1073/pnas.1602384113.

Ruosch, M., Spahni, R., Joos, F., Henne, P.D., van der Knaap, W.O., Tinner, W., 2016. Past and future evolution of *Abies alba* forests in Europe – comparison of a dynamic vegetation model with paleo data and observations. Glob. Ch. Biol. 22, 727–740. https://doi.org/10.1111/gcb.13075.

Sánchez-Salguero, R., Camarero, J.J., Gutiérrez, E., Gonzalez Rouco, F., Gazol, A., et al., 2017a. Assessing forest vulnerability to climate warming using a process-based model of tree growth: Bad prospects for rear-edges. Glob. Ch. Biol. 23, 2705–2719. https://doi.org/10.1111/gcb.13541.

Sánchez-Salguero, R., Camarero, J.J., Carrer, M., Gutiérrez, E., Alla, A.Q., et al., 2017b. Climate extremes and predicted warming threaten Mediterranean Holocene firs forests refugia. Proc. Natl. Acad. Sci. USA 114, E10142–E10150. https://doi.org/10.1073/pnas.1708109114.

Sangüesa-Barreda, G., Camarero, J.J., Oliva, J., Montes, F., Gazol, A., 2015. Past logging, drought and pathogens interact and contribute to forest dieback. Agric. For. Meteorol. 208, 85–94. https://doi.org/10.1016/j.agrformet.2015.04.011.

Shishov, V.V., Tychkov, I.I., Popkova, M.I., Ilyin, V.A., Bryukhanova, M.V., Kirdyanov, A. V., 2016. VS-oscilloscope: A new tool to parameterize tree radial growth based on climate conditions. Dendrochronologia 39, 42–50. https://doi.org/10.1016/j.dendro.2015.10.001.

Spinoni, J., Vogt, J.V., Naumann, G., Barbosa, P., Dosio, A., 2018. Will drought events become more frequent and severe in Europe? Int. J. Climatol. 38, 1718–1736. https://doi.org/10.1002/joc.5291.

Thornthwaite, C.W., 1948. An approach toward a rational classification of climate. Geogr. Rev. 38, 55–94.

Tinner, W., Colombaroli, D., Heiri, O., Henne, P.D., Steinacher, M., Untenecker, J., Valsecchi, V., 2013. The past ecology of *Abies alba* provides new perspectives on future responses of silver fir forests to global warming. Ecol. Monogr. 83, 419–439. https://doi.org/10.1890/12-2231.1.

Tumajer, J., Begović, K., Čada, V., Jenicek, M., Lange, J., Mašek, J., Kaczka, R.J., Rydval, M., Svoboda, M., Vlček, L., Treml, V., 2023. Ecological and methodological drivers of non-stationarity in tree growth response to climate. Glob. Chang. Biol. 29, 462–476. https://doi.org/10.1111/gcb.16470.

Tychkov, I.I., Sviderskaya, I.V., Babushkina, E.A., Popkova, M.I., Vaganov, E.A., Shishov, V.V., 2019. How can the parameterization of a process-based model help us understand real tree-ring growth? Trees-Struct. Funct. 33, 345–357. https://doi.org/10.1007/s00468-018-1780-2.

Vaganov, E.A., Hughes, M.K., Shashkin, A.V., 2006. Growth dynamics of tree rings: Images of past and future environments. Springer, Berlin, New York.

Vicente-Serrano, S.M., Camarero, J.J., Zabalza, J., Sangüesa-Barreda, G., López-Moreno, J.I., Tague, C.L., 2015. Evapotranspiration deficit controls net primary production and growth of silver fir: Implications for Circum-Mediterranean forests under forecasted warmer and drier conditions. Agric. For. Meteorol. 206, 45–54. https://doi.org/10.1016/j.agrformet.2015.02.017.

Vigo, J., Ninot, J., 1987. Los Pirineos. In: Peinado, M., Rivas Martínez, S. (Eds.), La vegetación de España. Universidad Alcalá de Henares, Alcalá de Henares, Spain, pp. 349–384.

Vitali, V., Büntgen, U., Bauhus, J., 2017. Silver fir and Douglas fir are more tolerant to extreme droughts than Norway spruce in south-western Germany. Glob. Ch. Biol. 23, 5108–5119. https://doi.org/10.1111/gcb.13774.

Vitasse, Y., Bottero, A., Rebetez, M., Conedera, M., Augustin, S., Brang, P., Tinner, W., 2019. What is the potential of silver fir to thrive under warmer and drier climate? Eur. J. For. Res. 138, 547–560. https://doi.org/10.1007/s10342-019-01192-4.

Wigley, T.M., Briffa, K.R., Jones, P.D., 1984. On the average value of correlated time series, with applications in dendroclimatology and hydrometeorology. J. Appl. Meteorol. Climatol. 23, 201–213.

Williams, A.P., Allen, C.D., Macalady, A.K., Griffin, D., Woodhouse, C.A., et al., 2013. Temperature as a potent driver of regional forest drought stress and tree mortality. Nat. Clim. Chang. 3, 292–297. https://doi.org/10.1038/nclimate1693.

Zang, C., Hartl-Meier, C., Dittmar, C., Rothe, A., Menzel, A., 2014. Patterns of drought tolerance in major European temperate forest trees: climatic drivers and levels of variability. Glob. Ch. Biol. 20, 3767–3779. https://doi.org/10.1111/gcb.12637.

Zweifel, R., Sterck, F., Braun, S., Buchmann, N., Eugster, W., Gessler, A., Etzold, S., 2021. Why trees grow at night. New Phytol. 231, 2174–2185. https://doi.org/10.1111/nph.17552.